Characterizing canopy complexity of natural and restored intertidal oyster reefs (*Crassostrea virginica*) with a novel laser-scanning method

Running Head: Investigating surface complexity on oyster reefs

Authors: David J. Cannon[a*], Kelly M. Kibler[a], Jyotismita Taye[a], Stephen C. Medeiros[b]
[a]Department of Civil, Environmental, and Construction Engineering and National Center for Integrated Coastal Research, University of Central Florida, Orlando, FL 32816, USA
[b]Department of Civil Engineering, Embry-Riddle Aeronautical University, Daytona Beach, FL 32114, USA
*Corresponding Author: djcannon@umich.edu

Author Contributions
KMK, SCM, DJC conceived and designed the research; KMK, SCM collected the observations; DJC, SCM performed data analysis; DJC, KMK, JT, SCM wrote and edited the manuscript

Abstract
The structural complexity of oyster reef canopy plays a major role in promoting biodiversity, balancing the sediment budget, and modulating hydrodynamics in estuarine systems. While oyster canopy structure is both spatially and temporally heterogeneous, oyster canopies are generally characterized using simple first-order quantities, like oyster density, which may lack the ability to sufficiently parameterize reef roughness. In this study, a novel laser scan approach was used to map the surface of intact reference and restored reefs (restoration age: 1 – 4 years) during low tide, when the oyster canopy was fully exposed. Measurements were used to estimate hydrodynamically-relevant roughness characteristics over the entire reef surface (>140 m^2; 0.50 m resolution), providing estimates of the canopy height (h_c), standard deviation (σ_c), rugosity index (R), and fractal dimension (D). Average canopy heights ranged from 3.6 – 4.9 cm, with canopy height standard deviations between 1.4 and 2.0 cm. Mean rugosity indices and fractal dimensions were relatively low on the youngest (1 year) restored reef (R=1.21; D=2.67), with substantial increases observed for more mature reef canopies (4 years: R=1.51; D=2.71). Structural complexity was consistently greater on reef margins than in reef interiors. Increases in complexity were linked to restoration age, with older reefs exhibiting more complex oyster canopies. The highest fractal dimension was observed on the intact reference reef, highlighting the importance of sustained reef growth for maintaining higher-order structural complexity. Results provide spatially explicit surface roughness characterizations for healthy, intertidal oyster reefs, with applications in both restoration science and natural and nature-based feature design.

Keywords: estuary, canopy, complexity, laser scan, oyster, roughness

Implications for Practice
- Typically measured oyster canopy characteristics, including live oyster density and shell length, are insufficient for accurately describing surface roughness on intact and restored reefs.
- The canopies of restored intertidal oyster reefs become more structurally complex over time, and proper restoration techniques can produce surface roughness characteristics that match or exceed those found on intact reference reefs.
- The spatially explicit canopy characteristics described in this study can be used to inform design of natural and nature-based features, especially those designed to provide ecosystem services controlled by surface complexity (e.g. habitat provision, wave attenuation, etc.).

Introduction

Oysters are considered "ecosystem engineers", so-called for their capacity to alter the physical, biological, and chemical signatures of the environment they inhabit (e.g. Morris et al. 2019) in a process of niche construction (Post & Palkovacs 2009). Habitat alteration occurs through a combination of (1) filter-feeding and waste deposition, which enhances water quality (Dame et al. 1989; Filippini et al. 2022) and sequesters carbon and nutrients (Chambers et al. 2018), and (2) reef-building, which is linked to shoreline stabilization (Meyer et al. 1997; McClenachan et al. 2020), current and wave attenuation (Cannon et al. 2022a), and habitat provision (Coen & Luckenbach 2000). Living oysters build complex three-dimensional structures, with reefs composed of branching clusters made up of mature living oysters, dead oyster shells, and newly recruited oyster spat (Figure 1b,c). These structures form a rigid canopy, composed of hundred (or thousands) of individual oyster clusters on the reef surface. Oyster canopies attenuate flows (Kitsikoudis et al. 2020), provide refuge for prey species (Peterson et al. 2003), and subsequently enhance biodiversity on the reef (Loch et al. 2021), with research suggesting that ecosystem benefits are directly linked to the structural complexity of the canopy itself (e.g. Hill & Weissburg 2013; Humphries et al. 2011; Soniat et al. 2004).

Over the last century, exogenous pressures have precipitated large declines in the global oyster population (>85% loss: Beck et al. 2011), and oyster-mediated ecosystem services have been simultaneously lost in affected coastal habitats. In recent years, coastal management has targeted construction and restoration of oyster reef habitat to recover these lost services, with research focused on effective strategies for recruiting oysters to natural reef or engineered reef-mimic structures (Goelz et al. 2020; Nitsch et al. 2021; Walters et al. 2021). Although restoration efforts have successfully recruited live oysters, a global meta-analysis of faunal abundance and diversity concluded that even successfully restored historical reef systems carry a considerable recovery debt as compared to pre-disturbed conditions (Hemraj et al. 2022). This recovery debt includes ecosystem services that may permanently lost, even after living oysters are re-introduced to the reef. An even more challenging task is the creation of new self-sustaining reef using artificial structures, an activity that has gained traction as a nature-based coastal defense aimed at slowing erosion (Morris et al. 2020). In a reef creation scenario, site environmental conditions and larval abundance may be less optimal as compared to sites of known historical reef. Focusing the design of artificial reef-like structures toward enhancing the recruitment and retention of target species

may improve long-term success in transforming artificial structures into living reef. In particular, the role of structural complexity on the reef surface has not been investigated. Oyster canopies are expected to change in height and complexity over time, especially on recently restored or constructed reefs where the canopy is actively growing, and structure-related ecosystem services may develop over relatively long timescales (Cannon et al. 2022b; La Peyre et al. 2014). While understanding the temporal development of canopy structure is imperative for evaluating the success of oyster reef restoration efforts, parameterizing the structural complexity of natural intact reef canopies is an equally important baseline for the design of natural and nature-based reef mimic structures.

Although the structural complexity of many marine (coral: Leon et al. 2015; Zawada & Brock 2009; mussel: Commito & Rusignuolo 2000) and terrestrial (forest: Atkins et al. 2018; Franklin & Van Pelt 2004) canopies have been studied extensively over the last several decades, studies of intertidal oyster reefs are relatively rare (exceptions: Margiotta et al. 2016; Karp et al., 2018). When reported, oyster reef canopy characterizations are generally restricted to estimates of the mean canopy height, living oyster density, and shell length as averaged over relatively few randomly selected points on the reef surface (e.g. Garvis et al. 2015; Walters et al. 2021; etc.). These measurements require intensive manual sampling, but they do not provide the spatial resolution required to describe an entire reef canopy or to estimate higher-order structural complexity parameters (e.g. rugosity, fractal dimension). However, the structural characteristics of intertidal oyster reefs provide unique opportunities for roughness measurements. The crest elevation of healthy oyster reefs is biologically mediated, and canopies experience full inundation and full exposure during high and low tide, respectively. While direct manual measurements may be extremely labor intensive, especially on large reef flats, low-tide exposure allows for indirect methodologies, like terrestrial laser scanning, to provide novel, high-resolution canopy measurements over the entire reef surface.

This study investigates the structural complexity of intertidal eastern oyster (*Crassostrea virginica*) canopies on intact reference and restored reefs in Mosquito Lagoon, Florida (USA). This work utilizes a space-for-time (SFT) approach to examine differences in reef characteristics related to restoration age, or time since restoration, with measurements collected 1-, 2- and 4-years post-restoration. We hypothesize that structural complexity will increase over time on restored

oyster reefs, with changes in canopy height, canopy height standard deviation, rugosity, and fractal dimension linked to restoration age. Furthermore, we hypothesize that oyster canopies may be more structurally complex than other rigid biological marine canopies (i.e. corals, mussels), which often lack the rough branching structures, length scale variability, and high element densities associated with intertidal oyster reefs. A novel method is proposed for characterizing canopy structure and roughness using a portable laser scanner, typically restricted to use in terrestrial settings. High-resolution laser scans were collected at low tide to help parameterize the structural complexity of oyster canopies on large reef flats (surface area: 144 – 440 m^2) at relatively small spatial scales (0.25 m^2 computation grids). The results and analysis presented herein are among the first of their kind, providing valuable insight for coastal managers restoring natural reef habitats and engineers designing natural and nature-based coastal infrastructure that utilizes living oyster canopy.

Methods

Study area

Measurements were collected in Mosquito Lagoon, a biologically diverse subtropical estuary on the Atlantic coast of Florida (USA). Mosquito Lagoon is generally shallow (mean depth: 1 m) and microtidal, with seasonal water level fluctuations on the order of $\pm$ 50 cm. Tidal exchange with the Atlantic Ocean occurs through Ponce de Leon Inlet (tidal amplitude: $\pm$ 100 cm), which is positioned at the northernmost tip of the waterbody. Study sites were located approximately 15 km southeast of the inlet, where tidal amplitudes were 20 - 30 cm. The northern portion of the lagoon, including the study area, is characterized by a complex network of channels that flow through a maze of sandy shoals, mangroves, and salt marsh wetlands (Figure 1; Mehta & Brooks 1973). This study is focused on intertidal oyster (*Crassostrea virginica*) reefs, which are abundant in the northern reach of the lagoon where tidal amplitudes are high enough to promote periodic inundation (e.g. Garvis et al. 2015). Intertidal reef is a dominant landscape feature throughout this region, and oysters occupy the margins of mangrove wetlands and form extensive reefs on the shallow shoals between vegetated islands.

Laser scans were conducted in the summer of 2018 on four intertidal oyster reefs in northern Mosquito Lagoon (Figure 1; Table 1). This work uses a space-for-time (SFT) approach to investigate changes in the structural complexity of intertidal oyster reef canopies over time. Instead

of following the evolution of a single restored reef as it matures over years (or decades), multiple reefs of increasing restoration age are used to infer how oyster canopies may change over time. Measurements were collected on an intact reference-condition reef (Reference), as well as three restored reefs defined by their year of restoration: R-2014, R-2016, and R-2017. These restored reefs can also be defined using their restoration age, or time since restoration, where R-2017, R-2016, and R-2014, are approximately 1 year, 2 years, and 4 years old, respectively. As a consequence of the SFT study design, it is assumed that differences in observed reef canopy structure are largely linked restoration age, with only minor variability associated with reef identity. Further consideration of potential reef identity effects can be found in the discussion.

Identical restoration techniques were employed at each restored reef, as detailed in Garvis et al. (2015). Prior reef degradation was linked to recreational boating in the lagoon, with boat wakes acting to dislodge oyster clusters and pile disaggregated shells into mounds at the reef crest (Grizzle et al, 2002). Degraded reef crest elevations were initially lowered to match nearby intact reefs, and extruded polyethylene mesh (Vexar^{TM}) oyster mats (size: 0.5 x 0.5 m) were anchored to the reef surface using concrete weights. Each mat was constructed using 36 adult *C. virginica* shells distributed across the surface of the mat and attached vertically to mimic the structure of live reefs. These mats promoted natural oyster recruitment at the restored reefs, and live oyster densities at each site were similar to those observed on reference reefs within one year of restoration (Cannon et al. 2022a).

Field measurements

Surveys were conducted to estimate canopy characteristics on each study reef. Manual canopy characterizations are labor intensive and measuring the entire reef surface (surface area: 150 – 450 m^2) is impractical. Instead, five 0.25m^2 sample quadrats were chosen on each reef to provide representative sample areas. Quadrat locations were selected haphazardly at low tide when the reef surface was exposed. Live oyster densities and shell lengths were estimated directly by counting and measuring all live *C. virginica* greater than 5mm in length in each quadrat. Individual quadrat measurements were used to compute reef-wide averages, medians, and standard errors. On each reef, a single quadrat was randomly selected and used to characterize the canopy height and canopy element density, defined as the total number of solid canopy elements, or oyster clusters, attached to the reef surface. Individual canopy elements were typically composed of both live and dead

oysters, as seen in Figure 2b. The mean canopy height and standard error were estimated by measuring the height of all canopy elements in the randomly selected quadrat, with heights measured from the reef surface to the highest point on the oyster cluster.

High-resolution canopy measurements were captured in detail using a FARO x330 terrestrial laser scanner. Although terrestrial laser scanners are more typically used for geospatial surveying in engineering operations, recent studies have demonstrated successful applications in complex biological structures, including forests (Wang et al. 2021) and blanket bogs (Chico et al. 2019). The FARO x330 is a phase-based laser scanner (pulse wavelength: 155 nm) with a maximum range of 330 m and a ranging error of $\pm$2 mm. The laser scanner was set to scan at maximum resolution, collecting 976 kpts/s at a step size of 0.009°, resulting in a point spacing of 1.5 mm at a distance of 10 m from the scanner. Laser scanning was completed at low tide during seasonal low water levels, ensuring that reef surfaces were maximally exposed. The laser scanner was deployed and repositioned multiple times on each reef to minimize the effects of shadows, which were created by individual canopy elements blocking the laser. Fixed spherical targets installed on tripods were used as reference points for aligning multiple scans, which were combined to produce a final point cloud for surface roughness analysis. Measurement positions were chosen such that the distance between the scanner and any individual target intended to remain in place for a subsequent scan position on a reef was never greater than approximately 10 m.

Data analysis

Laser scan data were initially imported and processed using FARO Scene Version 6. The key processing step is the registration (integration) of the multiple reef scans using the spherical targets that remained fixed for multiple scans. Data were filtered to remove erroneous stray points caused by dust and water vapor in the atmosphere. All measurements beyond the emergent edge of the reef, where the water surface intersected the reef canopy, were also removed. All point data were then exported to Matlab, where reef scans were subdivided into 0.25 m^2 computations grids (50 cm x 50 cm) for further analysis. All computation grids with fewer than 2500 points (mean density: 1 point/cm^2) were removed from analysis, as were all grids where the point bounding area (i.e. area of polygon bounding all points in grid cell) was less than 0.19 m^2, or 75% of the total grid area, resulting in between 20 and 40% data reduction for each reef. Removed grid cells were largely (>90%) located along reef fringes, where fluctuating water levels led to inconsistent laser

194 measurements. This quality control helped reduce computational errors due to edge effects and
195 low sampling densities.

196 In order to focus the analysis on oyster canopy structure, large-scale elevation changes related to
197 the underlying bed morphology were removed from the point cloud (Figure 2). For each sub-
198 sampled computation grid (50 cm x 50 cm), a plane was fit (least-squares) to the lowest 25% of
199 points selected from each of 16 equally distributed cells (12.5 cm x 12.5 cm) within the larger sub-
200 sample. The fit plane was then shifted to lowest measured elevation to represent the local sediment
201 surface, or bed-plane (Figure 2a). This procedure allowed identification of the bed for a large range
202 of point densities and bed slopes without relying on assumptions of spatial homogeneity in canopy
203 heights, as would be required for simple random sampling. All computation grids with maximum
204 bed slopes greater than 0.20 m/m were considered erroneous and removed from analysis.

205 All measured point elevations were converted to local canopy heights by subtraction from the bed-
206 plane. Elevations were then averaged over 1 cm x 1 cm grid cells to normalize point densities
207 across the measurement domain. This point density normalization was intended to reduce the
208 effects of measurement resolution on roughness characterizations, as has been discussed in
209 previous studies using manual measurement techniques (e.g. Knudby & LeDrew 2007). Although
210 the choice of horizontal grid resolution (1cm) was somewhat arbitrary, it is consistent with the
211 length of chain-links used in more high-resolution studies of coral canopy roughness (Knudby &
212 LeDrew 2007). Canopy height estimates in grid cells without points were set equal to zero, and
213 mean canopy heights (h_c) and canopy height standard deviations (σ_c) were estimated directly from
214 non-zero grid cell measurements, consistent with typical field measurement techniques.
215 Computation grids with average canopy heights greater than 15 cm were considered erroneous and
216 removed from analysis (based on in-situ observations), resulting in less than 2% total data loss.

217 The rugosity (R), or tortuosity index, for each computational grid was estimated as the ratio
218 between the surface area of the canopy (i.e. three-dimensional canopy-top) and the area of its
219 orthogonal projection onto the bed plane (i.e. flat reef surface: 0.25 m^2). Rugosity is a common
220 metric used for parametrizing biological roughness, especially in rigid canopies like coral reefs
221 (Shepard et al. 2001; Leon et al. 2015). In the current study, the canopy surface area was estimated
222 using a three-dimensional surface linearly interpolated between each non-zero canopy element in
223 the 0.5 x 0.5m grid (Figure 2b). The rugosity was defined as the total area of this irregular surface

divided by the area of the bed below the canopy (0.25 m^2). This methodology retained high spatial resolution while avoiding unrealistically sharp surface spikes associated with small interstitial areas in the canopy. The resulting surface is analogous to a sheet draped over the oyster canopy, and it is functionally similar to linear rugosity estimates, which rely on chain measurements with rigid links (length: 1 – 100 cm) which effectively filter out small-scale roughness elements (e.g. Knudby & LeDrew 2007).

The fractal dimension (D) of the oyster canopy was estimated from canopy height data using the variation method developed by Dubuc et al. (1989). The fractal dimension describes the complexity of an irregular surface, and it is strongly correlated with human visual perception of roughness (Pentland 1984). For three-dimensional surfaces, the fractal dimension ranges from 2 – 3, with higher values representing more complex surfaces. In this study, the fractal dimension was estimated following the methods described in Zhou & Lam (2005) and Zawada & Brock (2009). In short, a variable length window was defined for each computational grid (50 cm x 50 cm), with a side length $L=2\epsilon+1$ and 1 cm $\leq \epsilon \leq$ 12 cm. For each side length (3 – 25 cm), the window was positioned at all possible locations within the computational grid and the difference between the two most extreme within-window canopy height measurements (including zero-elements) was recorded and averaged to compute the mean variation $V(\epsilon)$. Finally, the best-fit slope (m) of the regression between $[V(\epsilon)]$ and $[\epsilon]$ was used to estimate the fractal dimension, defined as $D=3-m$. All computation grids with best-fit $R^2<0.85$ were removed from analysis, resulting in approximately 1% data loss.

Probability density functions (PDF) for all roughness variables (canopy height, canopy height standard deviation, rugosity, and fractal dimension) were estimated using a kernel density estimator, which provides a continuous, nonparametric estimate of the PDF without a priori assumptions about the distribution of the data (Bowman and Azzalini, 1997). PDFs were computed in Matlab using the *ksdensity* function with default bandwidth settings.

Results

Manually observed oyster characteristics varied across sample reefs, with live oyster densities and shell lengths that tended to increase with restoration age (Table 1). For restored reefs, live oyster densities (mean ± SE) ranged from 208 ± 7 oysters/m^2 (R-2016) to 475 ± 41 oysters/m^2 (R-2014). Although average oyster densities were lower on R-2016 (208 oysters/m^2) than on R-2017 (250

oysters/m^2), shell lengths were over 30% larger on the older reef (50.7 ± 1.2 mm vs. 37.6 ± 0.9 mm), reflecting the growth and replacement of first-year oyster recruits. The intact reference reef was characterized by lower live oyster densities (184 ± 34 oysters/m^2) and shorter shell lengths (40.5 ± 10 mm) than the oldest restored reef (R-2014). However, the number of rigid canopy elements (168 elements/m^2), which includes both live oyster and non-living reef structure, was nearly twice as large on the reference reef than on restored reef surfaces (84 - 96 elements/m^2).

Canopy heights (h_c) ranged from 3 – 10 cm, and reef-wide averages generally increased with restoration age (Table 1; Figure 3a-d; Figure 4a). Canopy heights at the youngest restored reef (R-2017) were smaller (mean $\pm$ 95% CI here and after: 3.6 $\pm$ 0.1 cm) than those measured at all other study sites, with shorter canopies presumably linked to the younger (~1 year), smaller oysters inhabiting the reef surface and the lack of accumulation of new oysters over multiple recruitment years. Accordingly, the tallest oyster canopies were observed at R-2014 (h_c: 4.9 $\pm$ 0.1 cm), where mean canopy heights in individual computation grids often exceeded 7 cm. In general, observed canopy heights were largest at the reef margins and decreased towards the center of the reef (Figure 5a). This trend was especially evident at R-2016, where spatial heterogeneity created a bimodal canopy height distribution in the probability density plot (Figure 4a). Importantly, manual measurements of canopy heights on each reef (Figure3a) generally fell within 0.5 cm of local laser-scan derived estimates (collected within 1m of quadrat), providing confidence in applied data-processing techniques.

Canopy height standard deviations (σ_c) followed trends observed in the mean canopy height (Table 1; Figure 3e-h), and larger standard deviations were observed on older reefs with taller canopies and higher densities of mature oyster. Reef-wide standard deviation averages ranged from 1.4 $\pm$ 0.1 cm at R-2017 to 2.0 $\pm$ 0.1 cm at R-2014. Following initial recruitment (R-2017), standard deviations increased on the reef margins (R-2016), widening the range of the distribution (Figure 4b; Figure 5b). As the reef continued to mature, additional oysters were recruited to the structure and distributions shifted to higher means (R-2014: 2.0 ± 0.1 cm). Canopy height standard deviations on the oldest restored reef (R-2014) were higher than those observed on the reference reef (Reference: 1.7 ± 0.1 cm), where estimates at the reef margins (1.9 ± 0.1 cm) were nearly 20% greater than those observed in the reef interior (1.6 ± 0.1 cm; Figure 5b).

Estimates of the rugosity index (R) ranged from 1.0 – 3.0, with an average rugosity of R = 1.37 ± 0.01 measured across all study reefs (Table 1; Figure 3j-m; Figure 4c). As with other roughness parameters, reef surface rugosity was linked to restoration age, increasing from 1.28 ± 0.08 at 1-year post-restoration (R-2017) to 1.56 ± 0.01 at 4-years post-restoration (R-2014). Mean rugosity estimates at R-2014 were higher than those measured at any other sample location, including the intact reference reef, where R=1.31 ± 0.01. Rugosity indices were spatially heterogeneous on the reference reef, with reef margins that were significantly rougher than the reef interior (Figure 5c) (R=1.39 ± 0.02 vs. R=1.28 ± 0.01).

Fractal dimension (D) estimates were consistent across study reefs, with reef-wide means between 2.67 and 2.74 (Table 1; Figure 3n-q, Figure 4d). The spatial distribution of fractal dimension (Figure 3n-q; Figure 5d) consistently highlighted complex reef margins, with less complexity in the reef interiors. The lowest fractal dimensions were observed in the interiors of the youngest study reefs (R-2017, R-2016), where fractal dimensions fell below 2.5 for ~5% of all computation cells. Probability density distributions (Figure 4d) narrowed with time since restoration, with a wider range of D observed on younger reefs. The fractal dimension was highest on the reference reef (D=2.74 ± 0.01), despite live oyster densities and canopy heights that were generally lower than those observed at R-2014.

Discussion

Roughness characteristics of intertidal oyster reef

Reef-scale roughness characteristics computed from the laser scan point clouds were similar to those described based on manual measurements of other natural marine canopies, including coral reefs (e.g. Knudky & LeDrew 2007; Leon et al. 2015; Miller et al. 2021), mussel beds (e.g. Commito & Rusignuolo 2000; Shynn Lim et al. 2020), and oyster reefs (e.g. Margiotta et al. 2016; Karp et al. 2018). Although direct comparisons are complicated by variable measurement techniques, which can have significant effects on inferred surface complexity (e.g. Yanovski et al. 2017; Knudly & LeDrew 2007), it is still useful to place the results of this study in the broader context of marine canopy literature. For example, rugosity indices on study reefs (range: 1.0 – 2.2) agreed well with those reported by Karp et al. (2018), Margiotta et al. (2015), and Rodney & Paynter (2006), who measured linear rugosity indices between 1.2 and 3.0 on restored and relic oyster reefs. On the other hand, the intertidal oyster reefs investigated in the current study were

markedly different than corals reefs, with prior studies reporting higher rugosity indices (Knudky & LeDrew 2007: 1 - 2.25; Burns et al. 2015: 1.5; Yanovski et al. 2017: 2.22; Carlot et al. 2020: 2 - 3.75) and lower fractal dimensions (Zawada et al. 2010: 2 - 2.5; Leon et al. 2015: 2.2 – 2.6; Miller et al. 2021: 2 – 2.5) for corals in comparison to oysters ($\overline{R}$=1.2 – 1.5; $\overline{D}$= 2.67 – 2.74). Differences in roughness characteristics between corals and oysters may be due, at least in part, to differences in reef growth and development. Intertidal oyster reefs develop through gregarious settlement of oyster larvae and individual oyster growth, creating complex, intertwining canopy structures composed of multiple age and size classes. Conversely, coral reefs predominantly develop through clonal colony growth, with many species producing large, relatively sparse canopy elements. These larger canopy elements are likely responsible for the higher rugosity indices reported for coral reefs, since the metric is defined based on *relative* changes in the canopy height compared to surrounding canopy elements. Higher fractal dimensions in oyster reefs may reflect the more random development process (i.e. larval attachment and growth), which produces characteristically irregular shells, sharp edges, and branching arms throughout the canopy. Additional studies focused on parallel measurements of oyster and coral reefs using identical methodologies may provide additional insight for differences in structural complexity between both marine canopies.

Temporal evolution of structural complexity on restored oyster reefs

In the current study, differences in canopy structure were well correlated with time since restoration, and older, more mature reefs were characterized by more complex surface structures. The observations presented here suggest that continued oyster recruitment and growth may increase surface complexity over several years post-restoration. All restored reefs started with no living oysters, and spat recruitment during the first season led to nearly immediate increases in live oyster density, canopy height, and canopy complexity (i.e. σ_c, R, D), as seen in R-2017. Following initial recruitment, living oysters continued to grow (i.e. increasing shell lengths) and the canopy developed distinct spatial patterns, with taller, more complex oyster clusters at the leading edge of the reef driving bimodal distributions in canopy height and canopy height standard deviation. The consistent patterns in spatial heterogeneity suggest that oyster spat may preferentially settle on the reef margins, at least during the early phases of reef development when growth is accelerated (i.e. Ridge et al. 2015). However, as similar patterns were also evident in the reference reef, spatial distributions may be linked to other ecological processes, including increased food availability (i.e.

nutrient concentration drawdown caused by filter feeding) and/or differential predation pressures. Following the first year of reef development, additional oyster growth and recruitment created increasingly complex canopy structures across the entire reef surface. The distributions of roughness characteristics narrowed and shifted to higher means, mirroring those observed on the intact reference reef within four years post-restoration. Ecosystem services moderated by canopy complexity, including habitat provision and energy (i.e. wave and current) attenuation, are expected to evolve simultaneously, as described in Cannon et al. (2022a,b). It is important to note that variability in surface complexity may also be linked, at least partially, to reef identity, with individual reef characteristics, including location, size, and sediment biogeochemistry, potentially playing a role in reef-to-reef canopy structure variability. While the study design (i.e. space-for-time) makes it difficult to distinguish between variability linked to restoration age and reef identity, the shared geological history and close proximity of the sample sites (i.e. within 3.5km) suggest that restoration age likely plays a larger role in modulating canopy evolution than variability in environmental factors.

The oldest restored reef investigated in this study (R-2014) matched or exceeded many surface roughness characteristics observed on the reference intact reef, suggesting that intertidal oyster reef restoration can be an effective method of recreating natural coastal infrastructure. The mean canopy height (4.9 ± 0.1 vs. 4.1 ± 0.1 cm), canopy height standard deviation (2.0 ± 0.1 vs. 1.7 ± 0.1 cm), and rugosity index (1.56 ± 0.01 vs. 1.31 ± 0.01) were all greater at the restored reef than at the reference reef. These differences in canopy characteristics mirror observed differences in (manually measured) live oyster density and shell length, suggesting that the restored reef also supported a larger, more abundant oyster population per unit area. However, the slightly elevated mean fractal dimension of the reference reef (2.74 ± 0.01 vs. 2.71 ± 0.01) indicates the prevalence of additional sources of three-dimensional complexity that are not captured by the canopy height and rugosity indices. Persistent historic colonization at the reference site has created a more fundamentally diverse canopy of live oysters and nonliving oyster shell structures, with complex branching surface structures built over centuries (or millenia) of oyster life cycles (recruitment, growth, decay) since the development of the barrier island ecosystem (~7000 years ago; Brooks 1972). For restored reefs, reaching a similar level of complexity, as measured by the fractal dimension, would likely take decades. The history of the reference reef also reflects human pressures. While the restored reefs are posted and protected from harvesting, fishermen can freely

harvest live oysters on the reference reef, where they generally target large, mature oysters over younger, smaller oysters, effectively reducing the live oyster density and shifting the distribution towards younger recruits. It is also possible that harvesting may have a direct impact on the structural complexity of the reef surface, with shifts in the size class distributions producing more (or less) complex oyster canopies over time. Although beyond the scope of the current work, additional research could help determine "optimal" harvest regulations for meeting and maintaining restored oyster reef complexity goals.

Applications to natural and nature-based feature design

Conventional infrastructure approaches alone are unlikely to effectively manage the hazards of flooding and erosion that threaten many coastal communities (Morris et al. 2020; Spalding et al. 2014). Engineered structures often disrupt sediment transport and accretion processes in coastal systems, exacerbating rather than ameliorating the effects of sea level transgression and more frequent strong storms (Temmerman et al. 2013). Adaptation plans that integrate natural features, such as oyster reefs, into multi-layered adaptation approaches are an attractive alternative to stakeholders given both their low cost and extensive provision of inter-related ecosystem services. Beyond incorporating living materials into designs, nature-based infrastructures depend on these organisms for performance-related processes, such as wave attenuation, sediment and carbon retention or self-repair. Investments to restore or create oyster reef, for example, may be selected to influence local hydrodynamic patterns, filter water and sequester carbon/nutrients, or create habitat complexity (Grabowski et al. 2012), with the expectation that the reef crest will self-adjust in response to disturbance and environmental changes. Each of these desired processes are related to specific attributes of the organism community. The ultimate hydrodynamic influence of a reef will be determined from the structural form of the reef and oyster canopy relative to the flow environment (e.g., Cannon et al. 2022b). The reef and canopy form in turn are shaped by a combination of material properties and ecological processes, including habitat tolerances and life history traits of oysters, as well as selective pressures of competition and predation.

The restored reefs featured in this study were notably successful from the perspective of recruiting oyster larvae, retaining spat, and promoting survival as evidenced by the healthy growth in oyster density, canopy height and complexity over time since restoration and the multi-generational size classes represented by varied shell lengths. The structural complexity of the oyster reef canopy

observed in this study relates directly to alteration of the near-reef flow field and to larval settlement and survival. For example, Cannon et al. (2022b) found that even as mean velocities within oyster canopy remained low, turbulent dissipation within oyster canopy increased many times over during a single year of oyster recruitment to a newly-restored reef. Drag coefficients estimated within complex reference-condition oyster canopy were two times greater than those observed on the surface of a degraded reef with no live canopy (Kitsikoudis et al. 2020) and an order of magnitude greater than those reported over bare sand and fine sediments (Styles 2015; Whitman & Reidenbach 2012). Notably, drag coefficients reported within oyster canopy also exceed those observed in shear layers that develop above the top of the canopy (Styles 2015), where Reynolds stresses peak and velocity profiles become logarithmic (Whitman & Reidenbach 2012).

It is likely that the differing hydrodynamic conditions observed within and above the oyster canopy work in tandem to attract and promote settlement of oyster larvae and then to retain and allow growth of spat. For example, larval *C. virginica* have been observed in lab studies to expend energy to propel themselves downward (e.g. dive) with greater frequency and force as turbulent dissipation rates increase (Fuchs et al. 2013; Fuchs et al. 2017). Turbulence created by the canopy may also signal larvae to swim to the bed and enhance the probability of settlement on established canopy structures (Fuchs & Reidenbach 2013). Additionally, high retention of spat settled within the relatively small spaces between shell or tile substrates (Whitman & Reidenbach 2012; Nestlerode et al. 2007; Lavan 2019) highlight the importance of interstitial niches of particular size for retention and survival. Whether the canopy niche size provides protection from predation or other physical habitat functions is unknown. Artificial reef created from materials that lack the complex 3-dimensional structure of natural reef canopy may fail to either recruit or retain larvae, and restoration design could include efforts to reproduce structural characteristics of natural, healthy reefs, as described in this work, to boost early colonization.

Acknowledgements

This work was funded by the U.S. National Science Foundation (NSF grants #1617374 and 1944880). We would like to thank Linda Walters and her research group for contributing biological oyster characteristics, including live oyster densities and shell lengths. We are also grateful to

Vasilis Kitsikoudis, David W. Spiering, and Barbara Nogueira Tirado for their help in field measurements. The authors declare that there is no conflict of interest.

References

Atkins JW, Fahey RT, Hardiman BS, Gough CM (2018) Forest canopy structural complexity and light absorption relationships at the subcontinental scale. *Journal of Geophysical Research: Biogeosciences* 123(4): 1387-1405

Beck MW, Brumbaugh RD, Airoldi L, Carranza A, Coen LD, Crawford C, Defeo O, Edgar GJ, Hancock B, Kay MC, Lenihan HS, Luckenbach MW, Toropova CL, Zhang G, Guo X (2011) Oyster reefs at risk and recommendations for conservation, restoration, and management. *BioScience* 61(2): 107-116

Bowman AW, Azzalini A (1997) Applied Smoothing Techniques for Data Analysis. New York: Oxford University Press Inc.

Breitburg DL (1999) Are three-dimensional structure and healthy oyster populations the keys to an ecologically interesting and important fish community? Pages 239-250 In: Luckenbach MW, Mann R, Wesson JA (eds) Oyster reef habitat restoration: a synopsis and synthesis of approaches. Virginia Institute of Marine Science Press, Gloucester Point, Virginia

Brooks HK (1972) Geology of Cape Canaveral. Pages 35-44 In: Garner TE (ed.). Space-age geology. Southeastern Geology Society. Tallahassee, Florida

Burns JHR, Delparte D, Gates RD, Takabayashi M (2015) Integrating structure-from-motion photogrammetry with geospatial software as a novel technique for quantifying 3D ecological characteristics of coral reefs. *PeerJ* 3, e1077

Cannon D, Kibler KM, Kitsikoudis V, Medeiros SC, Walters LJ (2022a) Variation of mean flow and turbulence characteristics within canopies of restored intertidal oyster reefs as a function of restoration age. *Ecological Engineering* 180, 106678

Cannon D, Kibler K, Walters LJ, Chambers L (2022b) Hydrodynamic and biogeochemical evolution of a restored intertidal oyster (*Crassostrea virginica*) reef. *Science of The Total Environment* 831, 154879

Carlot J, Rovere A, Casella E, Harris D, Grellet-Muñoz C, Chancerelle Y, Hedouin L, Parravicini V (2020) Community composition predicts photogrammetry-based structural complexity on coral reefs. *Coral Reefs* 39(4): 967-975

Chambers LG, Gaspar SA, Pilato CJ, Steinmuller HE, McCarthy KJ, Sacks PE, Walters LJ (2018) How well do restored intertidal oyster reefs support key biogeochemical properties in a coastal lagoon? *Estuaries and Coasts* 41(3): 784-799

Chico G, Clutterbuck B, Midgley NG, Labadz J (2019) Application of terrestrial laser scanning to quantify surface changes in restored and degraded blanket bogs. *Mires and Peat* 24(14): 1-24

Coen LD, Luckenbach MW (2000) Developing success criteria and goals for evaluating oyster reef restoration: ecological function or resource exploitation? *Ecological Engineering*, 15(3-4): 323-343

Commito JA, Rusignuolo BR (2000) Structural complexity in mussel beds: the fractal geometry of surface topography. *Journal of Experimental Marine Biology and Ecology* 255(2): 133-152

Dame RF, Spurrier JD, Wolaver TG (1989) Carbon, nitrogen and phosphorus processing by an oyster reef. *Marine Ecology Progress Series* 249-256

Dubuc B, Zucker SW, Tricot C, Quiniou JF, Wehbi D (1989) Evaluating the fractal dimension of surfaces. Proceedings of the Royal Society of London. A. Mathematical and Physical Sciences 425(1868): 113-127

Filippini G, Dafforn KA, Bugnot AB (2022) Shellfish as a bioremediation tool: A review and meta-analysis. *Environmental Pollution* 120614

Franklin JF, Van Pelt R (2004) Spatial aspects of structural complexity in old-growth forests. *Journal of Forestry* 102(3): 22-28

Fuchs HL, Hunter EJ, Schmitt EL, Guazzo RA (2013) Active downward propulsion by oyster larvae in turbulence. *Journal of Experimental Biology* 216(8): 1458-1469

Fuchs HL, Reidenbach MA (2013) Biophysical constraints on optimal patch lengths for settlement of a reef-building bivalve. *PLoS One* 8(8), e71506

Fuchs HL, Specht JA, Adams DK, Christman AJ (2017) Turbulence induces metabolically costly behaviors and inhibits food capture in oyster larvae, causing net energy loss. *Journal of Experimental Biology* 220(19): 3419-3431

Garvis SK, Sacks PE, Walters LJ (2015) Formation, movement, and restoration of dead intertidal oyster reefs in Canaveral National Seashore and Mosquito Lagoon, Florida. *Journal of Shellfish Research* 34(2): 251-258

Goelz T, Vogt B, Hartley T (2020) Alternative substrates used for oyster reef restoration: a review. *Journal of Shellfish Research* 39(1): 1-12

Grabowski JH, Brumbaugh RD, Conrad RF, Keeler AG, Opaluch JJ, Peterson CH, Piehler MF, Powers SP, Smyth AR (2012) Economic valuation of ecosystem services provided by oyster reefs. *BioScience* 62(10): 900-909

Grizzle RE, Adams JR, Walters LJ (2002) Historical changes in intertidal oyster (*Crassostrea virginica*) reefs in a Florida lagoon potentially related to boating activities. *Journal of Shellfish Research* 21: 749–756

Hemraj DA, Bishop MJ, Hancock B, Minuti JJ, Thurstan RH, Zu Ermgassen PS, Russell BD (2022) Oyster reef restoration fails to recoup global historic ecosystem losses despite substantial biodiversity gain. *Science Advances* 8(47), eabp8747

506 Hill JM, Weissburg MJ (2013) Habitat complexity and predator size mediate interactions between
507 intraguild blue crab predators and mud crab prey in oyster reefs. *Marine Ecology Progress*
508 *Series* 488: 209-219

509 Humphries AT, La Peyre MK, Decossas GA (2011) The effect of structural complexity, prey
510 density, and "predator-free space" on prey survivorship at created oyster reef mesocosms.
511 *PLoS One* 6(12), e28339

512 Hurst NR, Locher B, Steinmuller HE, Walters LJ, Chambers LG (2022) Organic carbon dynamics
513 and microbial community response to oyster reef restoration. *Limnology and*
514 *Oceanography* 67(5): 1157-1168

515 Karp MA, Seitz RD, Fabrizio MC (2018) Faunal communities on restored oyster reefs: effects of
516 habitat complexity and environmental conditions. *Marine Ecology Progress Series* 590:
517 35-51

518 Kitsikoudis V, Kibler KM, Walters LJ (2020) In-situ measurements of turbulent flow over
519 intertidal natural and degraded oyster reefs in an estuarine lagoon. *Ecological Engineering*
520 143, 105688

521 Knudby A, LeDrew E (2007) Measuring structural complexity on coral reefs. In: Pollock NW,
522 Godfrey JM (eds.) Diving for Science 2007. Proceedings of the American Academy of
523 Underwater Sciences 26th symposium 181-188

524 La Peyre MK, Humphries AT, Casas SM, La Peyre JF (2014) Temporal variation in development
525 of ecosystem services from oyster reef restoration. *Ecological Engineering* 63: 34-44

526 Lavan B (2019) Examining the effect of interstitial space on Eastern oysters (*Crassostrea*
527 *virginica*): Applications of photogrammetry and three-dimensional modeling. MS
528 Dissertation, James Madison University

529 Leon JX, Roelfsema CM, Saunders MI, Phinn SR (2015) Measuring coral reef terrain roughness
530 using 'Structure-from-Motion' close-range photogrammetry. *Geomorphology* 242: 21-28

531 Lim HS, Fraser A, Knights AM (2020) Spatial arrangement of biogenic reefs alters boundary layer
532 characteristics to increase risk of microplastic bioaccumulation. *Environmental Research*
533 *Letters* 15(6), 064024.

534 Loch JM, Walters LJ, Donnelly ML, Cook GS (2021) Restored coastal habitat can "reel in"
535 juvenile sportfish: Population and community responses in the Indian River Lagoon,
536 Florida, USA. *Sustainability* 13(22), 12832.

537 Locher B, Hurst NR, Walters LJ, Chambers LG (2021) Juvenile oyster (*Crassostrea virginica*)
538 biodeposits contribute to a rapid rise in sediment nutrients on restored intertidal oyster reefs
539 (Mosquito Lagoon, FL, USA). *Estuaries and Coasts* 44(5): 1363-1379

540 Margiotta AM, Shervette VR, Hadley NH, Plante CJ, Wilber DH (2016) Species-specific
541 responses of resident crabs to vertical habitat complexity on intertidal oyster reefs. *Journal*
542 *of Experimental Marine Biology and Ecology* 477: 7-13

McClenachan GM, Donnelly MJ, Shaffer MN, Sacks PE, Walters LJ (2020) Does size matter? Quantifying the cumulative impact of small-scale living shoreline and oyster reef restoration projects on shoreline erosion. *Restoration Ecology* 28(6): 1365-1371.

Mehta AJ, Brooks HK (1973) Mosquito Lagoon barrier beach study. *Shore Beach* 41: 27-34

Meyer DL, Townsend EC, Thayer GW (1997) Stabilization and erosion control value of oyster cultch for intertidal marsh. *Restoration Ecology* 5(1): 93-99

Miller S, Yadav S, Madin JS (2021) The contribution of corals to reef structural complexity in Kāne ʻohe Bay. *Coral Reefs* 40(6): 1679-1685

Morris RL, Bilkovic DM, Boswell MK, Bushek D, Cebrian J, Goff J, Kibler K, La Peyre MK, McClenachan G, Moody J, Sacks P, Shinn JP, Sparks EL, Temple NA, Walters LJ, Webb BM, Swearer SE (2019) The application of oyster reefs in shoreline protection: Are we over-engineering for an ecosystem engineer? *Journal of Applied Ecology* 56(7): 1703-1711

Morris RL, Boxshall A, Swearer SE (2020) Climate-resilient coasts require diverse defence solutions. *Nature Climate Change* 10(6): 485-487

Nestlerode JA, Luckenbach MW, O'Beirn FX (2007) Settlement and survival of the oyster Crassostrea virginica on created oyster reef habitats in Chesapeake Bay. *Restoration Ecology* 15(2): 273-283

Nitsch CK, Walters LJ, Sacks JS, Sacks PE, Chambers LG (2021) Biodegradable material for oyster reef restoration: First-year performance and biogeochemical considerations in a coastal lagoon. *Sustainability* 13(13), 7415

Pentland AP (1984) Fractal-based description of natural scenes. IEEE transactions on pattern analysis and machine intelligence. 6: 661-674

Peterson CH, Grabowski JH, Powers SP (2003) Estimated enhancement of fish production resulting from restoring oyster reef habitat: quantitative valuation. *Marine Ecology Progress Series* 264: 249-264

Post DM, Palkovacs EP (2009) Eco-evolutionary feedbacks in community and ecosystem ecology: interactions between the ecological theatre and the evolutionary play. Philosophical Transactions of the Royal Society B: Biological Sciences 364(1523): 1629-1640

Ridge JT, Rodriguez AB, Fodrie JF, Lindquist NL, Brodeur MC, Coleman SE, Grabowski JH, Theuerkauf EJ (2015) Maximizing oyster-reef growth supports green infrastructure with accelerating sea-level rise. *Scientific Reports* 5(1): 1-8

Rodney WS, Paynter KT (2006) Comparisons of macrofaunal assemblages on restored and non-restored oyster reefs in mesohaline regions of Chesapeake Bay in Maryland. *Journal of Experimental Marine Biology and Ecology* 335(1): 39-51

Shepard MK, Campbell BA, Bulmer MH, Farr TG, Gaddis LR, Plaut JJ (2001) The roughness of natural terrain: A planetary and remote sensing perspective. *Journal of Geophysical Research: Planets* 106(E12): 32777-32795

Soniat TM, Finelli CM, Ruiz JT (2004) Vertical structure and predator refuge mediate oyster reef development and community dynamics. *Journal of Experimental Marine Biology and Ecology* 310(2): 163-182

Spalding MD, Ruffo S, Lacambra C, Meliane I, Hale LZ, Shepard CC, Beck MW (2014) The role of ecosystems in coastal protection: Adapting to climate change and coastal hazards. *Ocean & Coastal Management* 90: 50-57

Styles R (2015) Flow and turbulence over an oyster reef. *Journal of Coastal Research* 31(4): 978-985

Temmerman S, Meire P, Bouma TJ, Herman PM, Ysebaert T, De Vriend HJ (2013) Ecosystem-based coastal defence in the face of global change. *Nature* 504(7478): 79-83

Walters LJ, Sacks PE, Campbell DE (2021) Boating impacts and boat-wake resilient restoration of the eastern oyster *Crassostrea virginica* in Mosquito Lagoon, Florida, USA. *Florida Scientist* 84(2/3): 173-199

Wang Q, Pang Y, Chen D, Liang X, Lu J (2021) Lidar biomass index: A novel solution for tree-level biomass estimation using 3D crown information. *Forest Ecology and Management* 499, 119542

Whitman ER, Reidenbach MA (2012) Benthic flow environments affect recruitment of *Crassostrea virginica* larvae to an intertidal oyster reef. *Marine Ecology Progress Series* 463: 177-191

Yanovski R, Nelson PA, Abelson A (2017) Structural complexity in coral reefs: examination of a novel evaluation tool on different spatial scales. *Frontiers in Ecology and Evolution* 5, 27

Zawada DG, Brock JC (2009) A multiscale analysis of coral reef topographic complexity using lidar-derived bathymetry. *Journal of Coastal Research* 10053: 6-15

Zawada DG, Piniak GA, Hearn CJ (2010) Topographic complexity and roughness of a tropical benthic seascape. *Geophysical Research Letters* 37(14)

Zhou G, Lam NSN (2005) A comparison of fractal dimension estimators based on multiple surface generation algorithms. *Computers & Geosciences* 31(10): 1260-1269

Tables

Table 1: Canopy characteristics as measured on restored (R-2017, R-2016, R-2014) and reference reefs. Measurements include reef area (m^2), live oyster density (oysters/m^2), live oyster shell length (cm), canopy height (cm), canopy standard deviation (cm), rugosity index, and fractal dimension. Mean and [median] canopy characteristics ($\pm$95% CI) were estimated over all grid cells (0.25 m^2) in a given reef area, while average ($\pm$ SE) live oyster densities and shell lengths were estimated from manual oyster counts on each reef. Measurements in curly brackets were manually measured using a single quadrat on each reef.

Reef Name	**Reef Area** m^2	**Live Oyster Density** oysters/m^2	**Live Oyster Shell Length** Mm	**Canopy Height** h_c; cm	**Canopy Standard Deviation** σ_c; cm	**Rugosity Index** R; unitless	**Fractal Dimension** D; unitless
R-2017	144	250 ± 13 {84 el/m^2}	37.6 ± 0.9	3.6 ± 0.1 [3.5 ± 0.1]	1.4 ± 0.1 [1.3 ± 0.1]	1.28 ± 0.03 [1.22 ± 0.02]	2.67 ± 0.01 [2.70 ± 0.01]
R-2016	326	208 ± 7 {96 el/m^2}	50.7 ± 1.2	4.0 ± 0.1 [4.2 ± 0.1]	1.5 ± 0.1 [1.4 ± 0.1]	1.32 ± 0.02 [1.27 ± 0.02]	2.69 ± 0.01 [2.70 ± 0.01]
R-2014	282	475 ± 41 {88 el/m^2}	58.8 ± 1.4	4.9 ± 0.1 [4.9 ± 0.1]	2.0 ± 0.1 [2.0 ± 0.1]	1.56 ± 0.01 [1.54 ± 0.01]	2.71 ± 0.01 [2.72 ± 0.01]
Reference	446	184 ± 34 {168 el/m^2}	40.5 ± 1.0	4.1 ± 0.1 [4.0 ± 0.1]	1.7 ± 0.1 [1.6 ± 0.1]	1.31 ± 0.01 [1.28 ± 0.01]	2.74 ± 0.01 [2.74 ± 0.01]

637

638 **Figure Captions**

639 Figure 1: (a) Map of study area with oyster reef locations displayed as colored squares (Reference:
640 green; R-2014: black; R-2016: magenta; R-2017: blue). Inset diagram shows the study area
641 location within Mosquito Lagoon, Florida, USA. Inset pictures highlight (b) typical canopy
642 element, or oyster cluster, composed of dead oyster shells and living oyster (c) intertidal oyster
643 reef and in-situ laser scan set-up, and (d) an example of raw point-cloud data collected on the reef
644 surface.

645 Figure 2: An example of processing steps for laser-scan analysis. (a) After sub-sampling raw
646 elevation data (sample area: 50 cm x 50 cm), a plane (red plane) was fit to the lowest 25% of points
647 (red points) selected from 16 equally-distributed grid cells (12.5 cm x 12.5 cm) and shifted to the
648 lowest elevation measured in the sub-sample (blue plane). (b) All points were converted to
649 elevation above plane (Z) and averaged over 1 cm x 1 cm grid cells, with the resulting canopy
650 heights used to fit a 3D canopy surface. The elevation of grid cells without sample points was set
651 equal to zero.

652 Figure 3: Spatial maps for reef structural complexity parameters as estimated from high-resolution
653 surface scans for restored (R-2017, R-2016, R-2014) and reference reefs. Parameters include the
654 mean canopy height (a-d), the standard deviation of the canopy height (e-h), the rugosity index (j-
655 m), and the fractal dimension (n-q). Reefs are drawn to scale, and horizontal and vertical tick marks
656 represent 10m intervals. Red boxes in (a) represent approximate locations for manual canopy
657 height measurement quadrats. Manually measured (*m*) and laser-scan (*ls*) derived canopy heights
658 are included for reference, with *ls* indicating the range of canopy heights estimated within 1m of
659 approximate quadrat locations.

660 Figure 4: Probability density plots comparing structural complexity parameters for restored (R-
661 2017: blue, R-2016: magenta, R-2014: black) and reference (green) reefs. Parameters include the
662 mean canopy height (a), the standard deviation of the canopy height (b), the rugosity index (c),
663 and the fractal dimension (d). Vertical lines are used to show the mean of each distribution (values
664 given in Table 1).

665 Figure 5: Distributions of observed canopy heights (a), canopy height standard deviations (b),
666 rugosity indices (c), and fractal dimensions (d) within 2 m of the edge (red) and in the center (blue)
667 of each reef (R-2017, R-2016, R-2014, Reference). Notches in boxplots represent 95% confidence
668 intervals on sample medians.

669

670

671

672

673

674

675

Figures

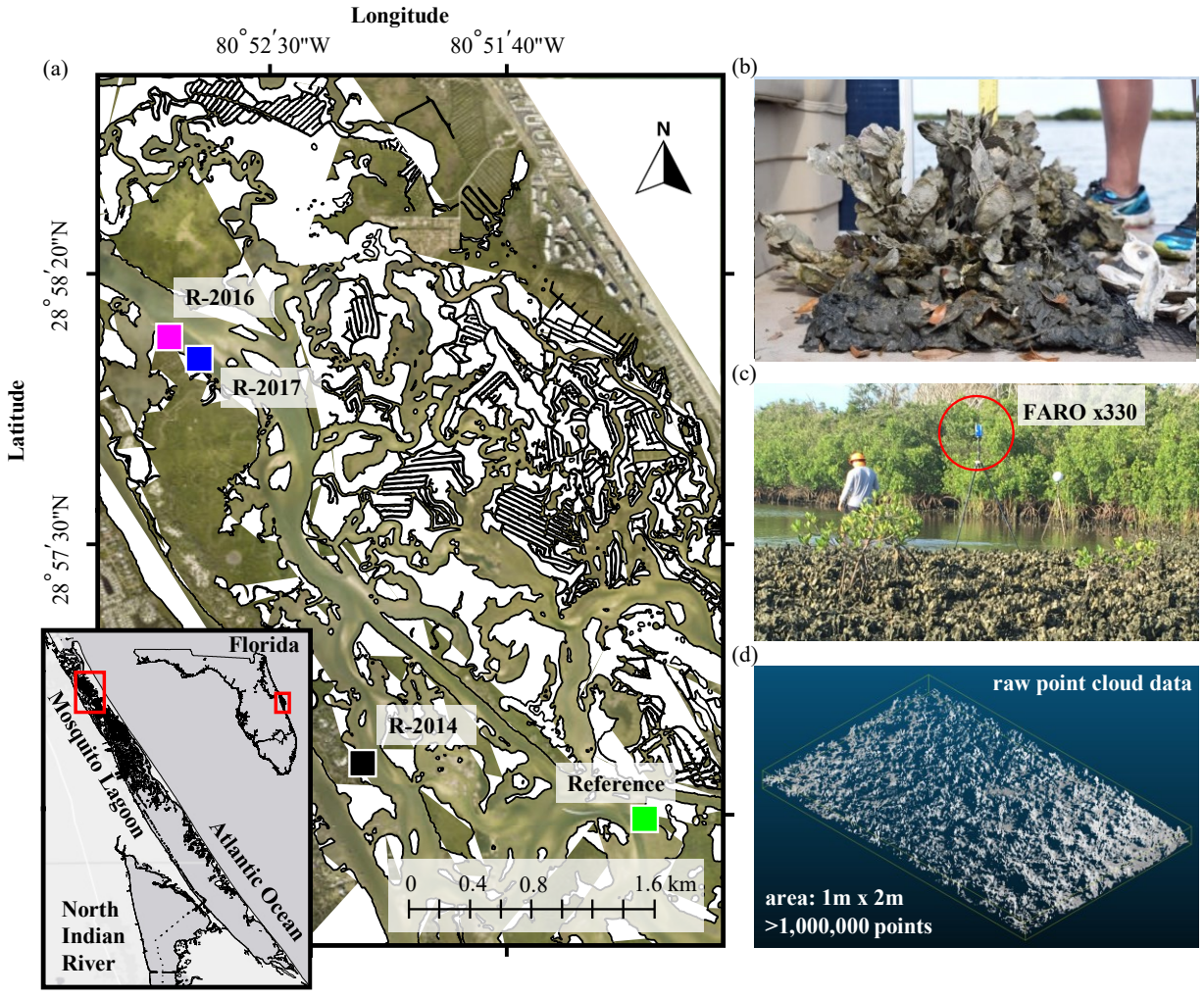

Figure 1.

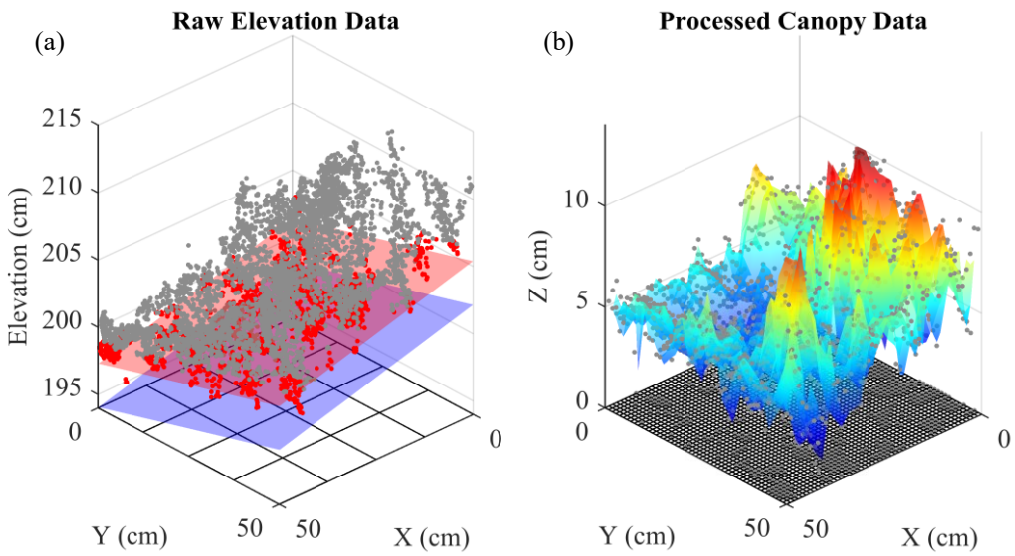
Raw Elevation Data
(a)
215
210
205
200
195
Elevation (cm)
0
Y (cm)
50
50
X (cm)
0
Processed Canopy Data
(b)
10
5
0
Z (cm)
0
Y (cm)
50
50
X (cm)
0

Figure 2.

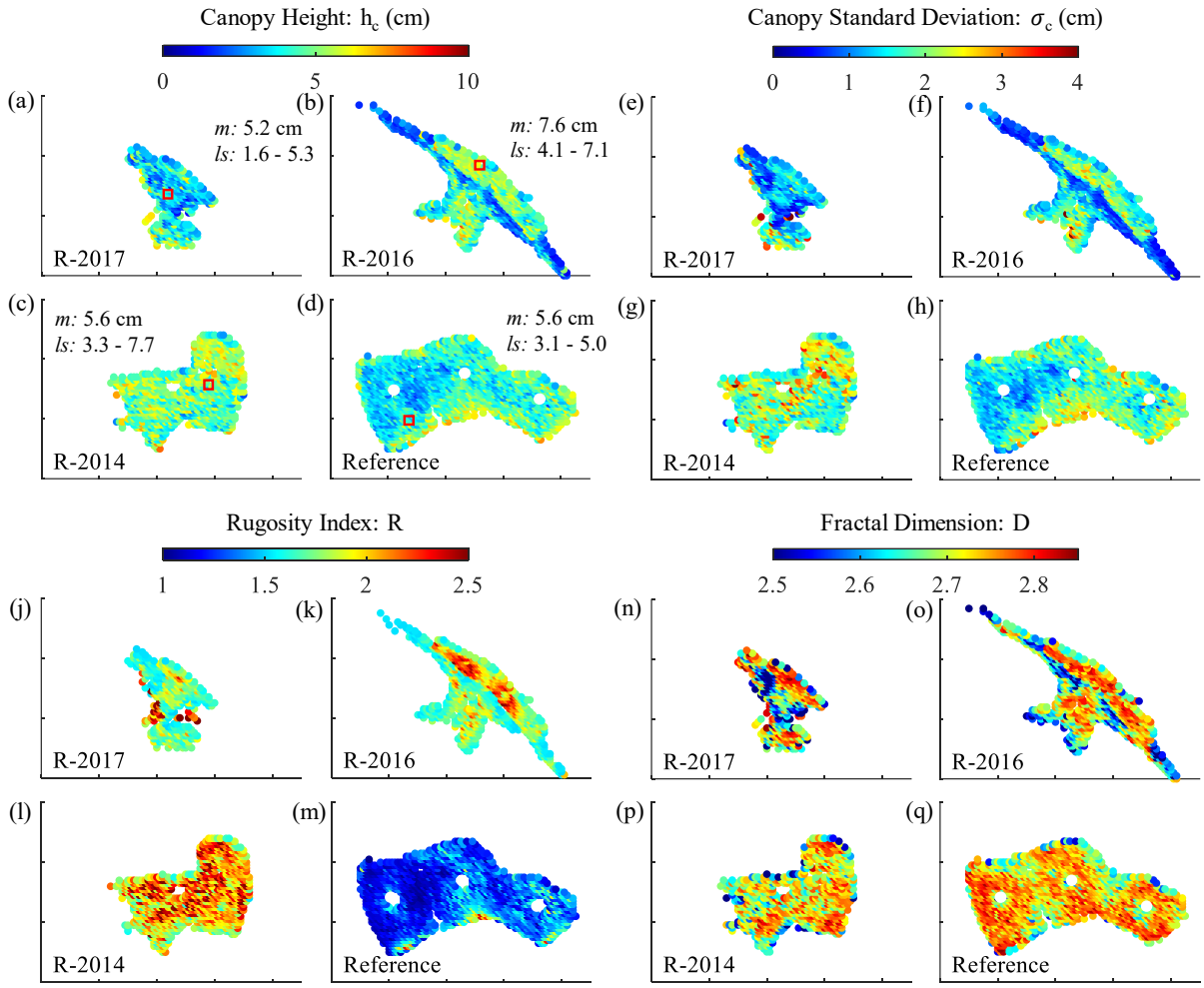
Canopy Height: h_c (cm)
0
5
10
(a)
(b)
m: 5.2 cm
ls: 1.6 - 5.3
m: 7.6 cm
ls: 4.1 - 7.1
R-2017
R-2016
(c)
(d)
m: 5.6 cm
ls: 3.3 - 7.7
m: 5.6 cm
ls: 3.1 - 5.0
R-2014
Reference
Canopy Standard Deviation: σ_c (cm)
0
1
2
3
4
(e)
(f)
(g)
(h)
R-2017
R-2016
R-2014
Reference
Rugosity Index: R
1
1.5
2
2.5
(j)
(k)
(l)
(m)
R-2017
R-2016
R-2014
Reference
Fractal Dimension: D
2.5
2.6
2.7
2.8
(n)
(o)
(p)
(q)
R-2017
R-2016
R-2014
Reference

Figure 3.

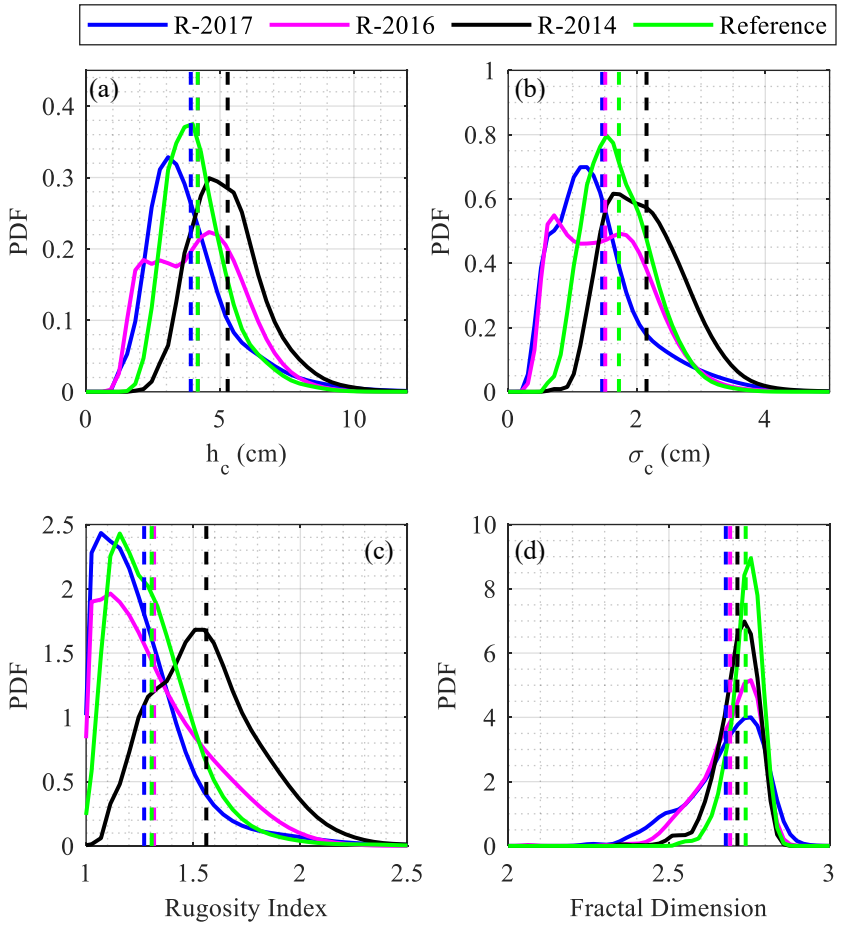
R-2017
R-2016
R-2014
Reference
(a)
(b)
(c)
(d)
PDF
h_c (cm)
σ_c (cm)
Rugosity Index
Fractal Dimension

Figure 4.

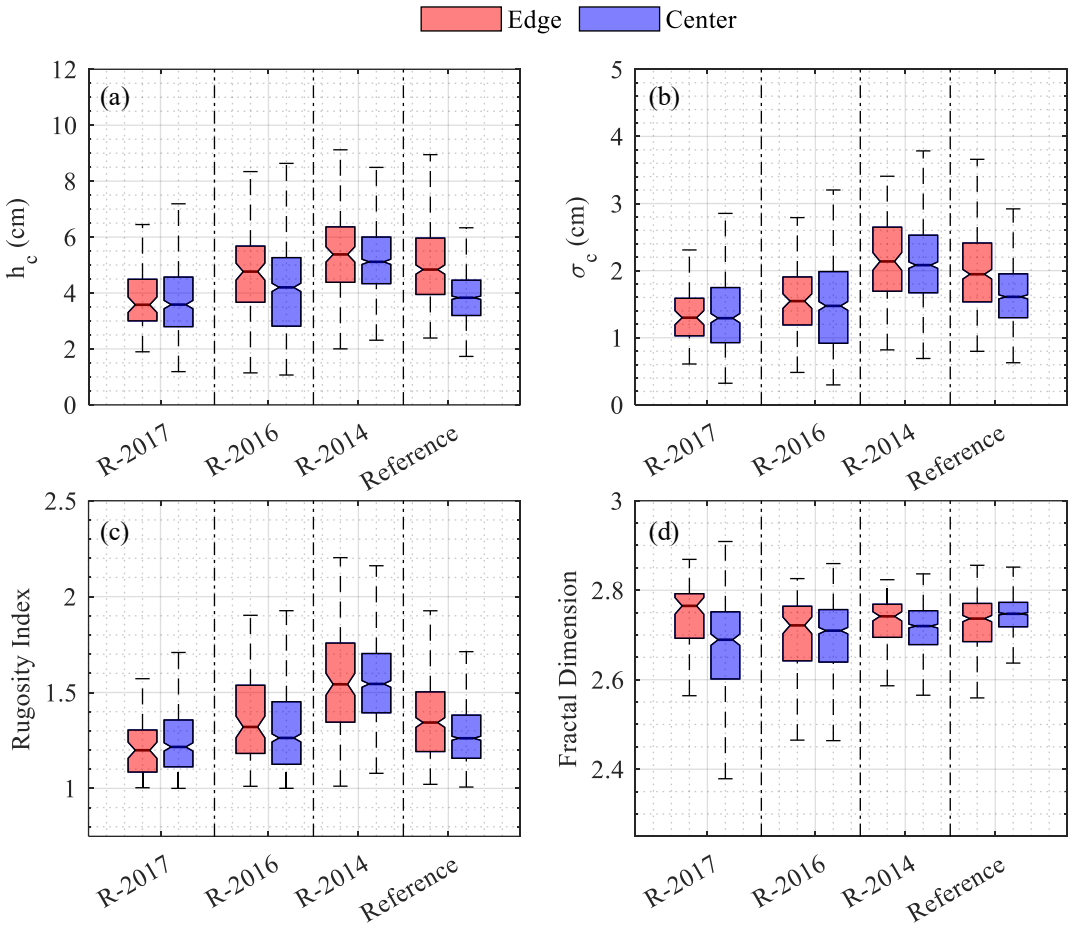

730

731 Figure 5.